

Comparison of Fast Frequency Response Methods in the Low-Inertia Grid of Cyprus

Andreas Argyrou, Savvas Panagi, Petros Aristidou

Sustainable Power Systems Laboratory, Department of Electrical Engineering, Computer Engineering and Informatics

Cyprus University of Technology, Limassol, Cyprus

anp.argyrou@edu.cut.ac.cy, {savvas.panagi, petros.aristidou}@cut.ac.cy

Abstract—Modern electric power systems with high levels of penetration of renewable energy sources (RES) often present frequency security problems. The lack of inertia due to the reduced number of synchronous generators in these systems, in combination with the usual inability of RES to provide frequency support, leads to system operators having to curtail RES or rely heavily on Under Frequency Load Shedding (UFLS) schemes to ensure frequency security. Fast Frequency Reserves (FFR) have been proposed as a solution to strengthen the frequency support of the system and alleviate security problems. FFR allows mitigating RoCoF, Nadir, and post-fault frequency steady-state problems after an event. In this paper, we present, analyze, implement and compare five FFR controllers to alleviate frequency security problems in low-inertia grids. The low-inertia, islanded, Cyprus dynamic model is used to quantify the results and exhibit the impact on a real system.

I. INTRODUCTION

Electrical energy is traditionally generated from primary energy sources such as coal, oil, water, or natural gas. These traditional power plants cause air pollution and greenhouse emissions when generating electricity. To meet the requirements of the Paris Agreement of a 40 percent reduction in carbon dioxide emissions by 2030, most countries replace a significant amount of synchronous generator generation with renewable energy sources (RES) [1]. However, this transition of electric power systems introduces challenges in frequency stability due to the high penetration of inverted-based resources [2].

While Synchronous Generators (SG) provide inertia to the system through their rotating masses, the power electronics which are used to connect the RES to the grid cannot provide inertia due to the lack of rotating parts [3]. Moreover, SGs provide additional frequency reserves to the system, which are important in significant disturbances. Hence, the high share of RES and, therefore, the reduction of conventional units in a power grid can lead to situations in which frequency control schemes will be driven to the limits and will not be able to prevent frequency deviations after a disturbance [4].

To overcome the challenges mentioned above, the utilization of Energy Storage Systems (ESS) and the design of appropriate battery management systems (BMS) to provide fast control reserves to the systems have been suggested [5]. More specifically, [6, 7] proposes a p-f droop controller that can adapt the active power output of the ESS proportionally to the frequency deviation. The authors of [2] state that

National Grid (UK) and EirGrid/SONI (Ireland) define fast frequency response services as a constant or a discrete step of output active power that is triggered when a certain frequency level is reached. The Rate of Change of Frequency (RoCoF) after a disturbance is a crucial parameter for assessing the robustness of an electrical grid and requires monitoring by system operators [8, 9]. Taking into consideration the above importance, a RoCoF droop controller (Virtual Inertia) and a static response once the RoCoF reaches a specified threshold have been proposed in [10] and [11] respectively to support the system.

The scope of the present work is to compare different fast frequency response methods. To achieve this, we implement five different fast frequency controllers within the dynamic model of the Cyprus power system using the DigSilent Power Factory software to study disturbances with variations in RES integration and load consumption.

The contributions of this paper are:

- The analysis of frequency response using different FFR control schemes, after a significant disturbance in several RES injection level and load consumption profiles.
- The advantages and disadvantages of each controller type.

This paper is structured as follows. In Section II, the crucial frequency parameters in a low inertia power system are described. In Section III, a brief explanation of the need for FFR and the five different FFR controller models are shown. Then, in Section IV the simulation results are discussed. Finally, conclusions are drawn in Section V.

II. FREQUENCY PROBLEMS IN LOW-INERTIA GRIDS

After a loss of generation event, critical frequency response characteristics such as Nadir, RoCoF, post-fault frequency steady-state value, and recovery time might endanger the stable operation of the network. To constrain all the aforementioned characteristics within secure limits, inertia and FCR reserves from conventional units play a pivot role in a traditional grid. The frequency response is also affected by both the size and the response time of FCR.

Today, with the increasing penetration of RES and, at the same time, the decommissioning of conventional units, the inertia and FCR reserves are also reduced. Hence, modern power systems face significant frequency stability problems as presented in Fig. 1. More specifically, the blue line depicts a disturbance scenario without RES, where RoCoF and Nadir

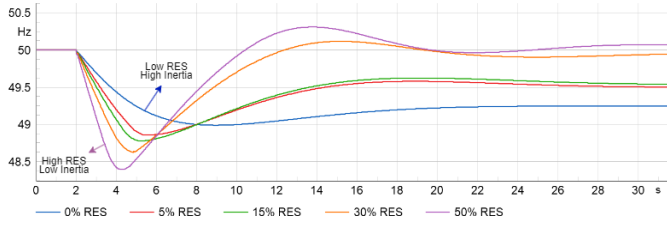


Fig. 1. Effects of Rising RES and Decreasing Inertia on Frequency Response Post Disturbance [13]

values are noticeably higher than the rest of the scenarios where there is an increase in RES penetration. The only advantage presented by scenarios with increased penetration of RES is the fast recovery of the system to the nominal frequency values. However, this is caused by the unwanted situation of UFLS protection activations. In addition, as the RES power increases, the UFLS activation stages increase, and at the same time more consumers are disconnected from the power grid to ensure safe operation.

The above effects of low Nadir are due to the response time between inertia and FCR reserves, although the available FCR size reserve may be sufficient. To address these consequences and bridge the gap between inertia and FCR activation time, fast frequency response (FFR) control via inverter-based resources must be employed. This reserve must be sufficient and fast enough to provide the necessary flexibility against changes in the level of power generation [12].

III. FAST FREQUENCY RESERVE CONTROLLERS

This section underscores the criticality of promptly managing frequency response using FFR controllers at the initial stages of an event. Subsequently, a brief explanation of five different FFR control methodologies is considered below.

A. Frequency Step Response

The block diagram of the frequency step response controller, currently used by [2], is shown in Fig. 2(a). It uses the frequency measurement as input, and when a specific threshold of frequency deviation is reached, BESS supplies a constant active power to the system for a specified duration. Typically, this duration aligns with the time required by the slowest generator connected to our grid to provide FCR support. Upon completion of the response period, the active power output of BESS will gradually decrease, allowing the entire system sufficient time to adjust to the new power balance.

The active power response of this controller is shown in Fig. 3(b) with the blue line. As seen, a step-change response in power is employed when the frequency drops below the threshold of 49.7Hz. The activation time takes less than 1 second to reach full output power due to the technical specification of ESS. Subsequently, the support duration lasts for 30 seconds. Finally, the deactivation process takes around 15 seconds, characterized by a constant slope power reduction.

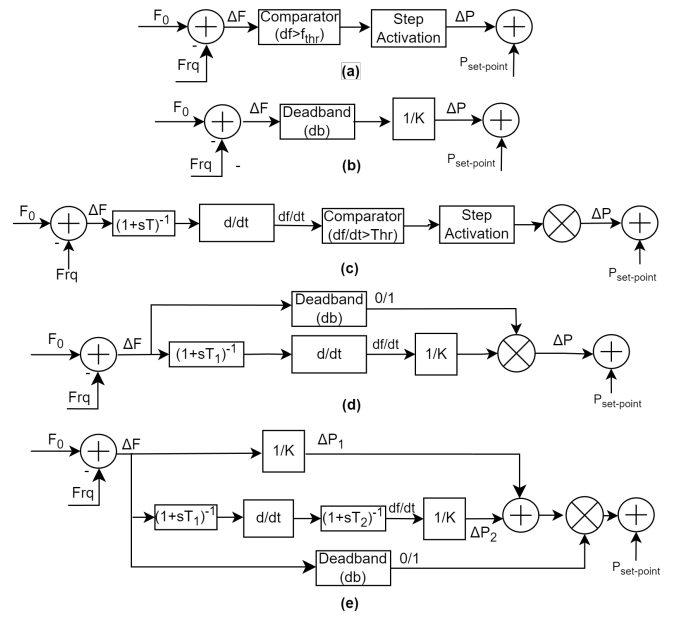


Fig. 2. Block diagram of FFR controllers, (a) frequency step, (b) frequency proportional, (c) RoCoF step, (d) virtual inertia, (e) Frequency-RoCoF proportional

B. Frequency Proportional Response

The frequency proportional control is presented in Fig. 2(b). When the frequency exceeds the deadband, the active power is either injected or absorbed proportionally to the frequency deviation until the frequency returns inside the deadband frequency range. This controller mirrors the conventional unit FCR response. The key distinction between them lies in the typically faster response time of the ESS. Figure 3(b) illustrates with a red line the output response of such a controller after a disturbance beyond the nominal range of 49.8Hz. When the frequency fails to return to the nominal frequency range, a small amount of power remains activated (steady-state error).

C. RoCoF Step Response

The RoCoF Step Response controller model is presented in Fig. 2(c). It is similar to the frequency step response, with the exception that the activation depends on the RoCoF threshold. This approach enables quicker recognition of abnormal power system disturbances, eliminating the need to wait for the frequency value to exceed the deadband limits. Consequently, a faster response time can be achieved [14].

Figure 3(b) illustrates with a green line the operation of FFR after a disturbance. The response of such a controller does not differ significantly from the frequency step response controller (blue line), as both operate on the same logic with the only difference being the trigger point mechanism. RoCoF step response is activated when the controller detects a RoCoF higher than a predefined threshold after a disturbance. The effectiveness of this approach depends on the selection of

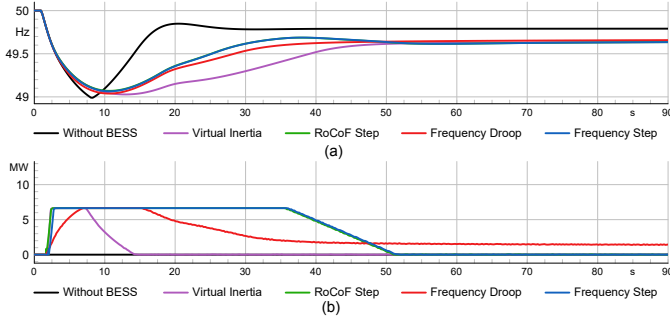


Fig. 3. Characteristics of the FFR controllers action, (a) Frequency response after loss of generation, (b) FFR power response

parameters, such as the time window (dt) for the calculation of the RoCoF and the threshold value of the RoCoF.

D. Virtual Inertia

Virtual Inertia generates an active power output that is proportional to the RoCoF as shown in Fig. 2(d). The primary objective is to minimize the RoCoF by adjusting the power [15]. Although inertia is associated with an immediate response to frequency changes, both grid-forming and grid-following inverter types can provide virtual inertia to the system. However, for the grid-following inverter to provide this reserve, a calculation of the RoCoF is required. Hence, a delay is inherent in the need for a frequency measurement. On the other hand, grid-forming inverters immediately provide the necessary power to the system during a frequency deviation [16]. In the current work, only grid-following inverters are discussed. Figure 3(b) represents in purple the output response of such a controller after a disturbance.

E. Frequency-RoCoF proportional

Taking into consideration the significance of fast response to minimize Nadir and at the same time the need to support power system frequency recovery to the nominal value, the combination between frequency proportional and virtual inertia controller is also proposed. The operation method remains consistent with those evaluated in the respective controllers. In Fig. 2(e) this type of controller is presented.

IV. IMPLEMENTATION AND EXPERIMENTAL RESULTS

In this section, each control method is implemented. To assess the effectiveness and application of each controller type, the functionality of each approach will be simulated across multiple disturbance scenarios, featuring various power system charging levels.

A. Test System Description

To evaluate the performance of each control type method, the Cyprus dynamic power system was used, implemented in the DiGSILENT Powerfactory software. The simplified diagram of the power system model is presented in Fig. 4. This system includes 26 generators, which include steam, gas and diesel power plants, together with 155 MW of wind farms

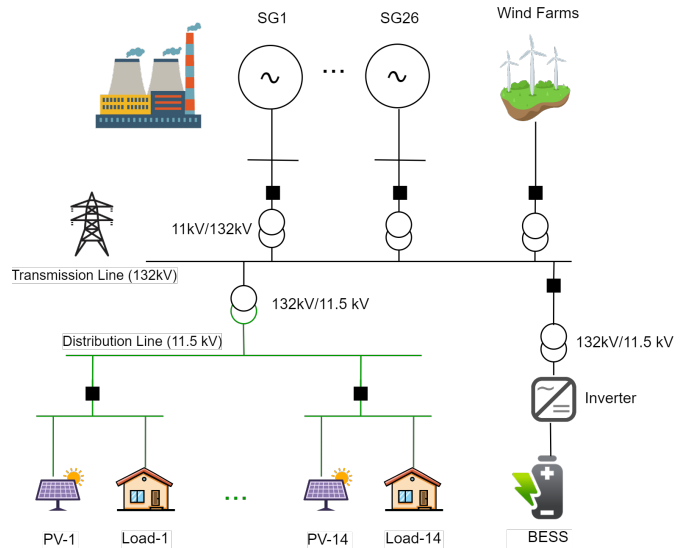


Fig. 4. Simplified Cyprus system diagram [19]

and around 656 MW of photovoltaic capacity [17, 18]. Distributed photovoltaic generation is connected in the distribution network with consumers, split into 14 groups. Each group is a different stage of UFLS activation protection. Finally, it incorporates an aggregated BESS with FFR capabilities. The dynamic model of the BESS is provided by DiGSILENT PowerFactory, with the FFR control model implemented by the authors, as depicted in Section III.

B. Analyzed Scenarios

In Table I, the values of the different loading levels considered in this paper are presented. The details of each scenario are presented in Table II. When the RES integration increases, the inertia and the FCR reserve from conventional generators is reduced. In addition, when the load increases, the inertia and FCR reserves increase. At the same time, the corresponding power due to the loss of the generator is increased.

TABLE I
CHARGING LEVELS FOR RES AND LOAD

Charging Levels	Power (MW)		
	Low	Moderate	High
RES	50	150	350
Load	575	825	1075

TABLE II
SCENARIO DETAILS AND SIMULATION RESULTS WITHOUT BESS

No. of Scenario	Load (MW)	RES (MW)	Disturbance (MW)	FCR (MW/0.5Hz)	Inertia (MWs)	Nadir (Hz)	RoCoF (Hz/s)
1	Low	Low	80	87	4164	48.97	0.38
2		Moderate		77	3709	48.89	0.43
3		High		77	3034	48.87	0.53
4	Moderate	Low	95	100	6754	49.01	0.28
5		Moderate		100	6602	48.99	0.32
6		High		95	5481	48.96	0.38
7	High	Low	110	118	9410	49.1	0.25
8		Moderate		118	8846	49.01	0.27
9		High		118	7273	48.98	0.31

C. Parameters

The frequency proportional controllers have a droop value of 0.01 pu / pu, to achieve maximum power activation in the frequency deviation of 50 ± 0.5 Hz. The Frequency-RoCoF droop controllers have a droop value of 0.01 pu/pu for both. The virtual inertia controller droop has been set to 0.002 pu/pu. The deadband has been defined based on the Cyprus grid code in the range of 50 ± 0.2 Hz. The target Nadir was set to 49 Hz, where the first UFLS protection stage is set. The frequency and RoCoF step response controller have activation thresholds at 49.7 Hz and 0.3 Hz/s respectively, with a support duration of 30 seconds and a deactivation time of 20 seconds for both.

In controller models that rely on the derivative of the frequency, a low-pass filter (LPF) is used to remove noise and generate a smooth response. The transfer function $(1 + sT)^{-1}$ represents the LPF, where T is the time constant and is related to the cutoff frequency [20]. Small values of the time constant lead to a faster measurement response, but to a more noisy signal. In contrast, large values result in a smoother output signal, but introduce substantial delay. In the virtual inertia controller, T_1 is set to 1 s to allow a contribution to the Nadir improvement. In RoCoF step response and Frequency- RoCoF droop controller, the T_1 and T_2 values were set to 0.15 s and 0.1 s, respectively.

D. Sizing of the BESS Capacity to Limit Nadir Value

First, the BESS capacity was chosen accordingly to achieve the target Nadir frequency of 49 Hz for each scenario. In this way, no UFLS protection is activated after the disturbances. The results are presented in Table III¹. Scenarios 4, 7, and 8 show no results (-) as their frequency Nadir remains above 49Hz without the need to activate FFR.

TABLE III
RESULTS WITH VARIABLE BESS CAPACITY

No. of Scenario	Nominal Power (MW)	Energy Consumption (MWh)	Nadir (Hz)
1	8.5/8/11/8/7.5	0.07/0.1/0.02/0.1/0.09	49
2	16/15.5/30/15.5/14.5	0.16/0.18/0.07/0.18/0.19	
3	17.5/17.5/30/17/16	0.16/0.2/0.07/0.2/0.21	
4	-	-	49.01
5	3.5/3.5/6/3.5/3.5	0.03/0.04/0.01/0.04/0.05	49
6	12/11/17/11/10.5	0.11/0.13/0.03/0.13/0.14	
7	-	-	49.1
8	-	-	49.01
9	9/8/15/8/8	0.09/0.1/0.03/0.09/0.11	49

E. Results with fixed BESS Capacity

In this section, the BESS power is set to a fixed value of 20MW to compare the effectiveness of each controller type under the same power capacity value. The results are presented in Table IV, while in Fig. 5 the frequency response for Scenario 9 is presented.

¹The values of each controller is presented with A/B/C/D/E, where A refers to the controller (frequency Proportional), B (frequency Step), C (Virtual Inertia), D (RoCoF Step), E (Frequency-RoCoF proportional).

TABLE IV
RESULTS WITH FIXED BESS CAPACITY 20MW

No. of Scenario	Energy (MWh) A/B/C/D/E	Nadir (Hz)
1	0.13/0.24/0.03/0.23/0.22	49.31/49.36/49.20/49.38/49.41
2	0.18/0.24/0.04/0.23/0.25	49.13/49.19/48.99/49.21/49.25
3	0.18/0.24/0.04/0.23/0.25	49.11/49.12/48.99/49.13/49.19
4	0.13/0.24/0.03/0.00/0.22	49.36/49.42/49.30/49.01/49.45
5	0.14/0.24/0.03/0.23/0.23	49.33/49.38/49.24/49.39/49.42
6	0.15/0.24/0.04/0.23/0.24	49.23/49.26/49.08/49.27/49.30
7	0.13/0.24/0.03/0.00/0.23	49.36/49.42/49.32/49.10/49.44
8	0.14/0.24/0.03/0.00/0.23	49.33/49.38/49.28/49.01/49.41
9	0.17/0.24/0.04/0.23/0.24	49.24/49.27/49.09/49.28/49.30

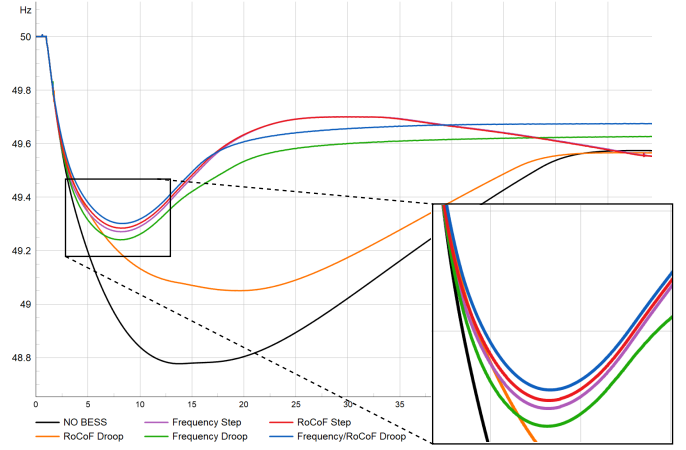


Fig. 5. Frequency response of Scenario 9 with a 20 MW fixed-capacity BESS

F. Discussions

Figure 5 illustrates the frequency response characteristics of each controller type, while, in Table V, all the capabilities of each methodology are summarized against their counterparts. These results are discussed below.

First, the experimental results indicate that each type of controller exhibits distinct advantages and limitations. Step response controllers and Frequency-RoCoF droop controllers raise the Nadir values; however, they require higher energy consumption relative to proportional controllers. Moreover, the RoCoF step controller exhibits the most rapid post-disturbance response times, while, as evidenced in scenarios 4, 7, and 8 in Table IV, it is adept at discerning when frequency deviations are negligible, thus preventing unnecessary activation.

As illustrated in Table III, the virtual inertia controller requires a substantially higher power input to maintain a frequency above 49 Hz compared to the other controllers. Furthermore, in the comparative analysis of the frequency proportional and RoCoF proportional controllers, it is evident that the latter offers minimal improvement to the Nadir and fails to provide adequate support during the frequency restoration phase, despite its rapid response. In contrast, the frequency proportional controller continues to provide support to the system until the frequency reaches the steady state.

Furthermore, the combination of Frequency-RoCoF droop controllers offers some of the positives of the corresponding

TABLE V
PERSPECTIVES FOR EACH CONTROLLER TYPE

Control Mode	Frequency Proportional (P-f)	Frequency Step	Virtual Inertia (P-df/dt)	RoCoF Step	Frequency-RoCoF Proportional (P-f,df/dt)
Improved Nadir	✓✓	✓✓✓	✓	✓✓✓	✓✓✓
Improved Initial RoCoF	Low	Low	Low	Low	Low
Improved Steady State	✓✓	✗	✗	✗	✓✓
Adaptive Response	✓	✗	✓	✗	✓
Energy Consumption	Moderate	High	Low	High	High
Symmetric Operation	✓	✗	✓	✗	✓

individual controllers while providing a longer support period, a better Nadir control, and a higher contribution of the storage unit to the FCR reserve.

Symmetric operation denotes the controller's capability to address both over-frequency and under-frequency scenarios within the system. Step controllers are limited to providing upward regulation, thereby rendering them asymmetrical. Furthermore, step controllers lack adaptability as, upon reaching the activation threshold, the FFR delivers a predetermined power output irrespective of the disturbance magnitude. Conversely, proportional controllers modulate the output power in accordance with the frequency deviation, enabling a more efficacious response to the event's significance.

The potential for enhancing the Rate of Change of Frequency (RoCoF) across various controller types is constrained due to the inherent latency in measurement, fault detection, and power regulation associated with grid-following inverters. Consequently, the initial RoCoF, generally observed within the first 500 milliseconds post-disturbance, remains largely unimproved.

V. CONCLUSIONS

This paper provides information on different types of FFR controller. The use of ESS for frequency control will be a valuable asset for low inertia system operators by reducing the activations of UFLS, and managing the frequency recovery to the nominal range. Each type of controller has different strengths and weaknesses, and based on the objectives that must be met, the appropriate controller must be selected.

ACKNOWLEDGMENT

The authors would like to thank Cyprus TSO for providing the dynamic model data.

REFERENCES

- [1] Y. Cheng, R. Azizpanah-Abarghoee, S. Azizi, L. Ding, and V. Terzija, "Smart frequency control in low inertia energy systems based on frequency response techniques: A review," *Applied Energy*, vol. 279, p. 115798, 2020.
- [2] L. Meng, J. Zafar, S. K. Khadem, A. Collinson, K. C. Murchie, F. Coffele, and G. M. Burt, "Fast frequency response from energy storage systems—a review of grid standards, projects and technical issues," *IEEE transactions on smart grid*, vol. 11, no. 2, pp. 1566–1581, 2019.
- [3] O. Dag and B. Mirafzal, "On stability of islanded low-inertia microgrids," in *2016 Clemson University Power Systems Conference (PSC)*. IEEE, 2016, pp. 1–7.
- [4] A. Ulbig, T. S. Borsche, and G. Andersson, "Impact of low rotational inertia on power system stability and operation," *IFAC Proceedings Volumes*, vol. 47, no. 3, pp. 7290–7297, 2014.

- [5] X. Li and S. Wang, "Energy management and operational control methods for grid battery energy storage systems," *CSEE Journal of Power and Energy Systems*, vol. 7, no. 5, pp. 1026–1040, 2021.
- [6] H. Zhu, H. Hong, J. Guo, Z. H. Chen, J. Wang, and C. Wang, "Frequency stability analysis and optimal control method in dg-bess microgrid system," in *2023 8th International Conference on Power and Renewable Energy (ICPRE)*, 2023, pp. 665–669.
- [7] K. S. El-Bidairi, H. D. Nguyen, T. S. Mahmoud, S. Jayasinghe, and J. M. Guerrero, "Optimal sizing of battery energy storage systems for dynamic frequency control in an islanded microgrid: A case study of flinders island, australia," *Energy*, vol. 195, p. 117059, 2020.
- [8] X. Deng, R. Mo, P. Wang, J. Chen, D. Nan, and M. Liu, "Review of rocof estimation techniques for low-inertia power systems," *Energies*, vol. 16, no. 9, p. 3708, 2023.
- [9] "Rate of Change of Frequency (RoCoF) withstand Capability," ENTSO-E, Tech. Rep., 2018.
- [10] W. Binbing, X. Abuduwayiti, C. Yuxi, and T. Yizhi, "Rocof droop control of pmsg-based wind turbines for system inertia response rapidly," *IEEE Access*, vol. 8, pp. 181 154–181 162, 2020.
- [11] P. V. Brogan, R. J. Best, D. J. Morrow, K. McKinley, and M. L. Kubik, "Effect of bess response on frequency and rocof during underfrequency transients," *IEEE Transactions on Power Systems*, vol. 34, no. 1, pp. 575–583, 2019.
- [12] L. T. Minh Trang and H. Nouri, "Modeling dynamic frequency control with power reserve limitations," in *2018 53rd International Universities Power Engineering Conference (UPEC)*, 2018, pp. 1–5.
- [13] S. Panagi and P. Aristidou, "Sizing of fast frequency response to improve frequency security in low-inertia power systems," in *preprint*, 2024. [Online]. Available: <https://engrxiv.org/preprint/view/3586/6636>
- [14] M. Nuhic and G. Yang, *Battery Energy Storage System Modelling in DIGSILENT PowerFactory*. Springer International Publishing, 2021, pp. 177–200.
- [15] R. Mandal and K. Chatterjee, "Virtual inertia emulation and rocof control of a microgrid with high renewable power penetration," *Electric Power Systems Research*, vol. 194, p. 107093, 2021.
- [16] A. Jalali, "Voluntary Specification for Grid-forming Inverters-May 2023-A statement of voluntary threshold," Australian Energy Market Operator, Tech. Rep., 2023.
- [17] EAC, TSOC. RES Hosting Capacity Capabilities. Accessed: 2024-03-31. [Online]. Available: <https://www.arcgis.com/apps/dashboards/134fdd8988d44ade8dd33b5c1c26ca65>
- [18] EAC. Generation Data. Accessed: 2024-03-31. [Online]. Available: <https://www.eac.com.cy/EL/EAC/Operations/Pages/Generation.aspx>
- [19] S. Panagi, A. Lazari, V. Koutsoloukas, and P. Aristidou, "Impact of fast frequency response on renewable energy source curtailment and load shedding," in *2024 CIRED Workshop*, Vienna, 2024.
- [20] J. Barrios-Gomez, F. Sanchez, G. Claudio, F. Gonzalez-Longatt, M. Acosta, and D. Topic, "Rocof calculation using low-cost hardware in the loop: Multi-area nordic power system," in *2020 International Conference on Smart Systems and Technologies (SST)*, 2020, pp. 187–192.